British Journal of Mathematics & Computer Science
10(2): 1-21, 2015, Article no.BJMCS.18555
ISSN: 2231-0851

SCIENCEDOMAIN *international*
www.sciencedomain.org

Design, Optimization and Fabrication of a Climbing Six Articulated-Wheeled Robot Using Artificial Evolution and 3D Printing

S. H. Lim[1] and J. Teo[1*]

[1]Evolutionary Computing Laboratory, Faculty of Computing and Informatics, Universiti Malaysia Sabah, 88400 Kota Kinabalu, Sabah, Malaysia.

Article Information

DOI: 10.9734/BJMCS/2015/18555
Editor(s):
(1) Doina Bein, Applied Research Laboratory, The Pennsylvania State University, USA.
Reviewers:
(1) Anonymous, Federal University, Brazil.
(2) Wagner Tanaka Botelho, Computation and Cognition, Federal University of ABC, Brazil.
(3) Anonymous, Portugal.
Complete Peer review History: http://sciencedomain.org/review-history/9920

Original Research Article

Received: 28 April 2015
Accepted: 13 June 2015
Published: 27 June 2015

Abstract

Over the last decade, various mobile robots have been developed and widely used in myriad sectors. However, the vast majority of mobile robots are manually designed where the designers must have the preliminary knowledge of the interaction between the robots with the environment. Additionally, the high complexity involved in the design of the kinematics and controllers of a mobile robot has always been the biggest challenge for the researchers and practitioners alike. Thus, the task of designing a robot can be considered very demanding and extremely challenging. In this research, an artificial evolution approach utilizing Single-Objective Evolutionary Algorithm (SOEA) and Multi-Objective Evolutionary Algorithm (MOEA) respectively are investigated in the automatic design and optimization of the morphology of a Six Articulated-Wheeled Robot (SAWR) with climbing ability. Results show that SOEA is able to produce optimized SAWR with climbing ability while MOEA is able to produce a set of Pareto optimal solutions which provide users with a choice of solutions for trade-off between the objectives of morphology size and climbing performance. The Pareto optimal set of solutions are the smallest SAWR with least climbing ability to biggest SAWR with the best climbing motion. The research continues by transferring the evolved solutions from simulation to the real world using 3D printing. The body, legs and wheels of the evolved robots are printed by a 3D printer and assembled with sensors, servos and motors for real world testing. Results show that the fabricated real world SAWRs are able to perform the climbing motion with the average accuracy of 85.8% in comparing to the performance in simulation.

Keywords: Articulated-wheeled robot; evolutionary robotics; 3D printed robots; climbing robots; hybrid mobile robots.

**Corresponding author: jtwteo@ums.edu.my, eohnuhs@outlook.com;*

Abbreviations

DOF : *Degree of Freedom*
DC : *Direct Current*
MEOA : *Multi-objective Evolutionary Algorithm*
RPM : *Rotation per Minute*
SAWR : *Six Articulated-Wheeled Robot*
SOEA : *Single-objective Evolutionary Algorithm*

1 Introduction

Since the first implementation of mobile robots in World War II, mobile robotics has become an extremely popular research topic. Mobile robotics can be utilized in a wide range of applications. For example, service industry, military deployments, manufacturing, cleaning, entertainment and remote exploration, especially in search and rescue operations where human lives can be endangered. Mobile robot can be traditionally categorized into two categories which are wheeled and legged mobile robots. Wheeled robots have the characteristic that they can traverse a longer distance with a faster speed with their wheels than legged robots. Besides that, wheeled robots are more powerful in terms of load/weight ratio [1]. However, wheeled robots generally having difficulties when traversing over a rough terrain i.e. with obstacles, steps, discontinuous contact surface, among others. On the other hand, legged robots provide a flexible adaptive mobility in unstructured environment and a better performance while traversing over rough terrain. In terms of travelling speed and power efficiency, legged robots are still falling behind of wheeled robots achievement.

A hybrid platform with the combination of leg and wheel has excellent maneuverability on flat ground and uneven terrain. Therefore, a hybrid platform is highly recommended for general indoor and outdoor environment operations as it is the trend for "future" mobile platforms [2]. In recent years, hybrid mobile robots have been designed for various functionality and purposes. For example, hybrid mobile robots designed for stairs climbing purposes, performing jumping behavior, in-situ reconfiguring robots posture and adapting to uneven terrain, among others. In general, hybrid mobile robots can carry out their mission better in rough terrain compared to traditional wheeled or legged mobile robots. Hybrid mobile robots utilize the advantages of both wheeled and legged mechanisms while compensating the downside of each other.

There are many successful examples of hybrid mobile robots which are built and designed for wide range of operations [3-9]. A group of researchers from a few universities in Japan had developed a hybrid wheeled-legged platform through a retracting mechanism inspired by the armadillo [10]. The idea of a retractable wheeled-legged module is that the specially-designed wheels can be transformed into a legs-like mechanism. Smith, Sharf and Trentini from McGill University proposed PAW, a four legs robot with wheels equipped at the end of each leg [11]. PAW is the first to combine wheeled mode locomotion with dynamically stable legged locomotion. The interested reader may refer to a more detailed review of hybrid mobile robots [12].

Numerous types of hybrid mobile robots have been proposed and developed. However, as far as we aware, most of the hybrid mobile robots are manually designed where the designers must have the preliminary knowledge of the interaction between the robots with the environment. Besides that, the extremely complexity in the kinematic and controller designing of a hybrid mobile robot has always been the biggest challenge for the researchers. Planning is an important aspect of the effort to design robots that perform their task with some degree of flexibility and responsiveness to the environment [13]. According to Akerka, planning is a difficult problem for a number of reasons, not the least of which is the size of the space of possible sequences of moves [13]. Even a simple robot which can only move forward, backward, right or left has so many different ways that the robot can possibly move around in an environment. On the other hand, manually morphology designed on trial-and-error basis is not guaranteed to be optimal from the large design space [14]. Thus, the task of designing a robot can be considered demanding [15], especially in designing a hybrid mobile robot. Here raises the research question on the ability of obtaining an optimized morphology

of a climbing SAWR with evolution approach. The robot described in this paper is referred to as SAWR with the ability to climb over obstacles while travelling with wheeled locomotion.

The use of artificial evolution for the automatic generation and synthesis of controllers and/or morphologies for robots is one of the more recent methods in developing robots [16-25]. By implementing evolutionary algorithms in designing a robot, an optimized controller and/or morphologies can be obtained where at times, these evolved solutions might be beyond the designers' design capability.

Successful examples of designing robots with artificial evolutionary approach, walking robots designed with evolutionary computation in optimizing the morphology and controller [26] and swarm robotics with their controllers designed by evolutionary algorithms with artificial neural networks [27]. Different from previous related researches, the morphology optimization of a climbing hybrid mobile robot, which is a six articulated-wheeled robot, is investigated in this research.

In this research, an artificial evolution method with single-objective and multi-objective evolution algorithm is proposed to design and optimize the morphology of a six articulated-wheeled robot (SAWR) with climbing ability. Instead of stopping the research after obtaining results from simulation, evolved solutions from simulation are transferred intro real world SAWRs and their performance in real world environment are investigated. The contribution of this research is to open up the implementation of artificial evolution methods in designing robots to a new category where a climbing hybrid mobile robot is involved in this study. Besides that, the realization of simulation solutions to real world robots with 3D printing technology in this research is highly promising and can be applied in future related works.

Section 2 describes the methodologies used in this research which includes the design of the SAWR with the climbing motion, evolutionary algorithms (SOEA and MOEA) and fabrication methodology. Section 3 presents the experimental setup in this research which includes the evolution with SOEA and MOEA and real world testing for the fabricated SAWRs. Besides that, the results for all experiments are also presented in Section 3. Lastly, the conclusion and suggestion of future works are outlined in the last section, Section 4.

2 Methodologies

In this research, a Six Articulated-Wheeled Robot (SAWR) has been designed and served as test bed. The locomotion mechanism of the SAWR allows a traditional leg robot to overcome their complex and slow walking mechanism by attaching wheels at the end of each leg. On the other hand, articulated-wheel mechanism allowed a traditional wheeled robot to traverse through rough terrain and further enhance the robot with climbing capability. Thus, the SAWR in this research is designed to have the capability to perform climbing motion.

2.1 SAWR and the Climbing Motion

The SAWR has six one degree-of-freedom (DOF) legs and the range of each leg joint is 180 degrees. An active wheel is attached to each leg of the SAWR. The main traversing method of the SAWR is based on wheel locomotion. While with the support of legs, the robot can reconfigure itself to perform climbing motion in order to overcome obstacles. The SAWR is actuated with twelve independent actuators where six for the legs and six for the wheels. There are two sensors integrated to drive the SAWR autonomously especially in obstacle negotiation ability.

Fig. 1 shows the front view and side of the SAWR. In the figure, s1 is representing the front sensor and s2 is representing the rear sensor. While b, l and w are the evolving parameters which are to be optimized in the evolution process in this research. The SAWR is designed to have the capability of climbing obstacles and steps in order to operate in a more complex environment. With two sensors and six active wheels where each are attached on one DOF legs, the SAWR can perform a sequence of reconfiguration motions to climb up and down from obstacles.

The original idea of the reconfiguration method for climbing upward and downward steps is obtained from Lu and Bu on their paper "Study on the Mobile Robot Reconfiguration Control Methods" [28]. They had proposed a series of reconfiguration method of a six legged-wheeled robot for ridges and channels negotiation. However, the reconfiguration method is enhanced in this research to sensors-based reconfiguration method. The robot with our proposed reconfiguration method can perform climbing motion autonomously based on the changes of values from the sensors onboard.

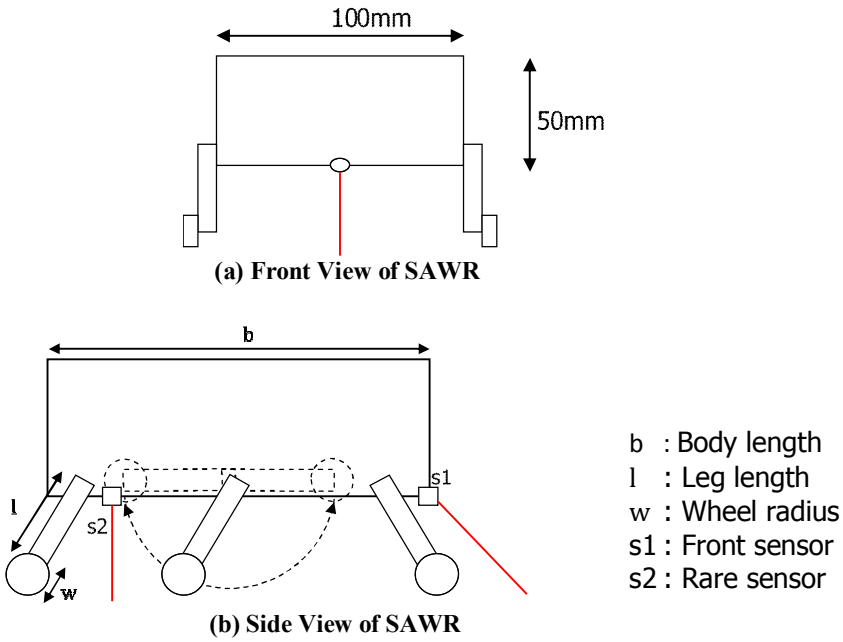

Fig. 1. Morphology design of the SAWR

The series of reconfiguration method of climbing upward step is shown in Fig. 2. Fig 2.1 shows the original marching position where the SAWR is moving forward. When the SAWR is approaching to obstacles, value from front sensor, s1 will be changed when the obstacle is detected by the sensor as shown in Fig. 2.2. The climbing reconfiguration method will be activated when obstacle is detected by sensor s1. Firstly, the SAWR will reconfigure itself as in Fig. 2.3 and continue move forward until the s1 sensor value is changed again as in Fig. 2.4. Then the SAWR is now ready to place both of the front legs down on the obstacle which can be seen in Fig. 2.5. After that, the SAWR will continue moving forward until the value of s2 sensor is changed as shown in Fig. 2.6. Then the SAWR will reconfigure itself by placing down the middle wheels on the obstacle as seen in Fig. 2.7. The SAWR will continue moving forward for a short duration and finally reconfigure itself back to the original marching position as shown in Fig. 2.8.

Fig. 3.1 shows the original marching position where the SAWR is moving forward. By referring to the value changes of sensor s1, SAWR can determine a downward step is approaching as shown in Fig. 3.2. Firstly, the SAWR will reconfigure itself as in Fig. 3.3 and continue moving forward. The SAWR will move forward until the front wheels goes off from the step for a certain distance, this can be determined by referring to the value changes of s1 sensor as shown in Fig. 3.4. After that, the angle of the front leg will be adjusted as in Fig. 3.5 and the robot will continue moving forward. By inspecting the value changes of s2 as shown in Fig. 3.6, the SAWR can determine whether the middle wheels are going off from the step and ready to reconfigure itself as in Fig. 3.7. Lastly, the SAWR will put down the rear wheels onto the ground after moving forward for a short period and the robot is recovered to the original marching reconfiguration as shown in Fig. 3.8.

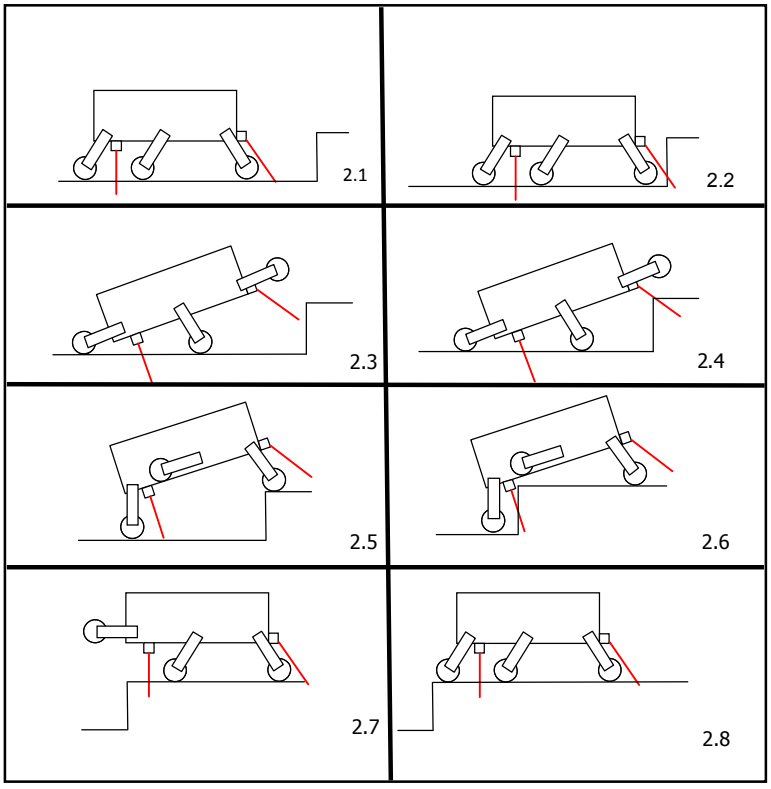

Fig. 2. Reconfiguration method of climbing upward step

Thus, the controller design for the SAWR in this research is designed according to the climbing up and climbing down reconfiguration methods. The controller of SAWR is only designed to move forward and reconfiguration methods of climbing up or down will be triggered when approaching upward steps or downward steps while the controller for the climbing upward step and downward step is designed based on the reconfiguration methods described above.

2.2 Evolutionary Algorithms

In this research, two evolutionary algorithms had been proposed which is the evolution method with the integration of Single-Objective Evolutionary Algorithm (SOEA) and Multi-Objective Evolutionary Algorithm (MOEA). SOEA is able to produce fittest climbing SAWRs with optimized/minimized morphology while MOEA is able to produce Pareto-sets of optimal solutions which are different sizes of SAWRs with different achievement in performing climbing motion in the task environment. This can provide users a choice of solutions for trade-off between the two objectives which are the size of the SAWR and the ability in performing climbing motion.

2.2.1 Single-objective evolutionary algorithm (SOEA)

Fig. 4 shows the flowchart of the SOEA. The SOEA starts with initializing population with random parameters for the SAWR body length, leg length, and wheel radius. Then the individual will be simulated in simulation to perform climbing motion and the performance of the individual will be evaluated. A fitness score will be calculated based on a fitness function which will be described later. The fitness score will be compared with the parent's fitness score. The parent will be abandoned and replace with the individual if the individual has better score than the parent. After that, parent will undergo mutation operation to produce

offspring for next generation if the maximum number of generation is not reached. New offspring will then be started again with the simulation to perform climbing motion and the process will repeat until the maximum number of generation is reached.

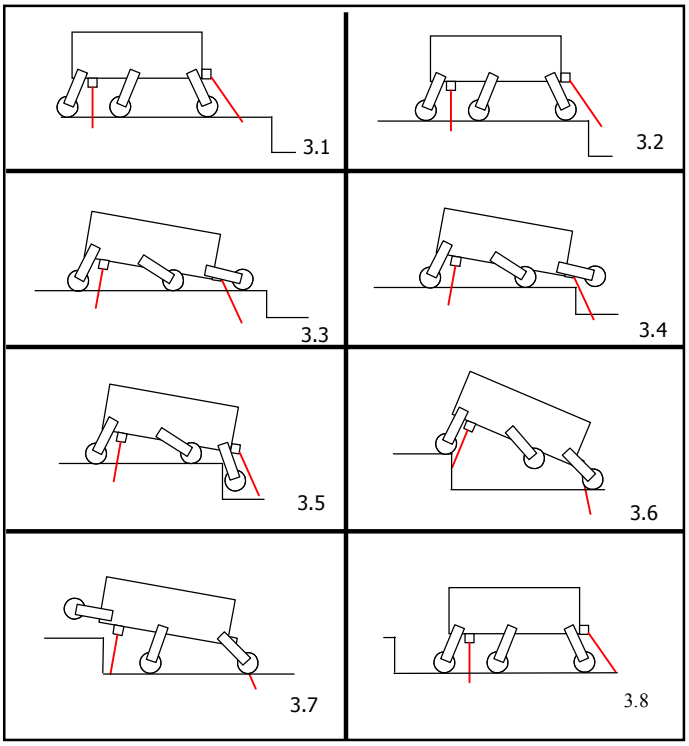

Fig. 3. Reconfiguration method of climbing downward step

Fitness function of the SOEA is shown in equation 1. The fitness function is designed as in the way that the lesser is the fitness score, the better it is. The first part of the fitness function is a direct addition of the SAWR body length with the SAWR leg length and the SAWR wheel radius to reflect the main objective of this research which is to obtain a smallest possible climbing SAWR.

$$\text{Fitness} = (b + l + w) \times (1 + d \times 10) + (c \div mc) \quad (1)$$

b = robot body length (mm);
l = robot leg length (mm);
w = robot wheel radius (mm);
d = robot final destination from target destination (m);
c = number of collision occurs during simulation;
mc = maximum number of collisions possible to occur during one simulation.

Besides that, the capability of the SAWR to perform climbing motion is also an important criterion in determining the fitness of a robot as a small SAWR without the capability of climbing obstacle is not a desired solution. Thus, the second part of the fitness function is to ensure individuals with the capability to perform climbing motion must be credited with better score in comparing to smaller individuals without the climbing capability. This can be achieved by taking the distance of the individual final position from the goal destination to multiply with ten in order to increase the weight. Then the value will be added by one before multiplying with the first part of the fitness function which is the size of the SAWR.

The last part of the fitness function is to penalize individuals that have collision with the obstacles during the simulation. The total number of collisions occurs during the simulation is divided by the maximum number of collision that is possible to occur in a single run of simulation in order to scale the penalize score with the fitness function. The maximum number of collisions is obtained in a preliminary experiment where the SAWR is purposely set to collide with an obstacle throughout the run.

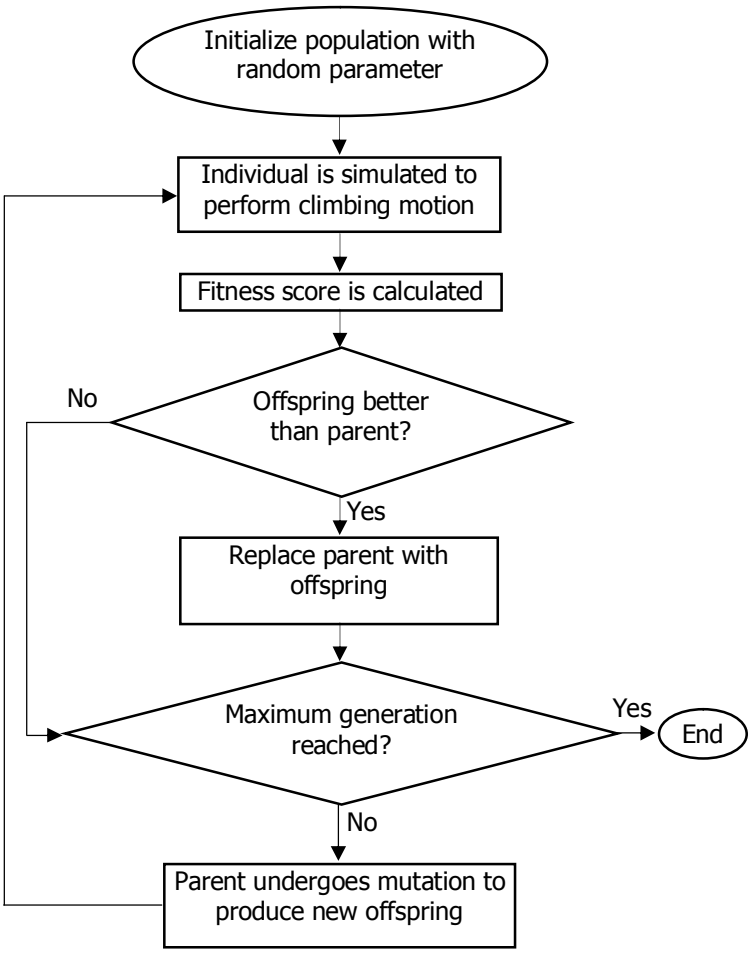

Fig. 4. Flowchart of the SOEA

Mutation is carried out after parent selection. The selected parent will undergo mutation operation in order to produce new offspring for next generation. In this research, a fixed, non-adaptive mutation operation is implemented. Mutation operation is an addition operation of the parent evolving parameters with Gaussian numbers (random numbers with mean of zero and standard deviation of one). Mutation operation will be done to the parent body length, parent leg length and parent wheel radius which are shown in Equations 2, 3 and 4.

$$\text{Offspring Wheel Radius} = PR + (G/3) \times (Rmax - Rmin) \quad (2)$$

$$\text{Offspring Leg Length} = PL + (G/3) \times (Lmax - Lmin) \quad (3)$$

$$\text{Offspring Body Length} = PB + (G/3) \times (Bmax - Bmin) \quad (4)$$

G = Random Gaussian number;
PR = Parent wheel radius;
$Rmax$ = Maximum value of wheel radius (40 mm);
$Rmin$ = Minimum value of wheel radius (15 mm);
PL = Parent Leg length;
$Lmax$ = Maximum value of leg length (100 mm);
$Lmin$ = Minimum value of leg length (35 mm);
PB = Parent body length;
$Bmax$ = Maximum value of body size (350 mm);
$Bmin$ = Minimum value of body size (200 mm).

2.2.2 Multi-objective evolutionary algorithm (MOEA)

Multi-objective evolutionary algorithm (MOEA) is used to solve problems that involve optimizing multiple objective functions simultaneously. In this experiment, MOEA is implemented in attempting to produce a set of Pareto optimal solutions in a single run. In our case, the Pareto set optimal solutions are different sizes of SAWR with different achievement in performing climbing motion in the task environment. This can provide users a choice of solutions for trade-off between the two objectives which are the size of the SAWR and the ability in performing climbing motion.

Fig. 5 shows the flowchart of the MOEA. The MOEA starts with initializing population with random parameters for the SAWR body length, leg length, and wheel radius. Then the individual will be simulated in Webots to perform climbing motion and the performance of the individual will be evaluated. There are two fitness functions in the MOEA which are the size fitness and performance fitness. Performance fitness will be scored by evaluating the performance of the individual in climbing obstacle while the size fitness will be scored based on the size of the morphology.

After both of the fitness scores have been credited, the individual will be compared to each member from the archive. If the individual is non-dominated where either one of the fitness score is better, the archive will be updated by adding the individual as a new member and also removing all the other dominated solutions. A parent will be randomly selected from the archive if the maximum number of generation is not reached. Selected parent will undergo mutation operation to produce new offspring for next generation. New offspring will then be started again with the simulation to perform climbing motion and the process will repeat until the maximum number of generation is reached.

In MOEA, distinct from SOEA, there are more than one fitness functions which are the objectives to be optimized simultaneously. In this research, there are two fitness functions in the MOEA which are the size fitness and performance fitness. Both of the fitness functions are designed as in the smallest is the value, the better is the score.

$$\text{Size Fitness} = b + l + w \tag{5}$$

b = robot body length (mm);
l = robot leg length (mm);
w = robot wheel radius (mm).

$$\text{Performance Fitness} = d^2 + (c \div mc) \tag{6}$$

d = robot final destination from target destination (m);
c = number of collision occurs during simulation;
mc = maximum number of collisions possible to occur during one simulation.

Equation 5 shows the first fitness function, size fitness. Size fitness is built up with the summation of three parameters which are the body length of SAWR, leg length of SAWR and wheel radius of SAWR. Thus, SAWR with bigger morphology will have higher value of fitness score which is poorer. On the other hand, smaller SAWR will be credited better fitness score which is score with lower value.

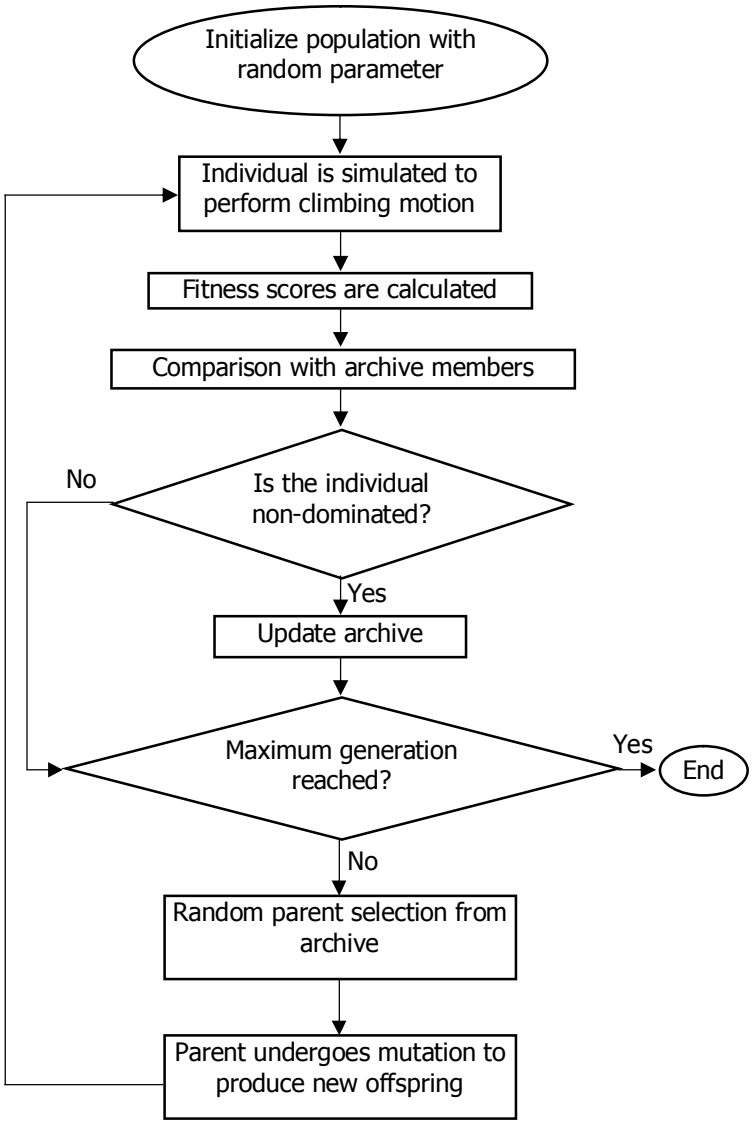

Fig. 5. Flowchart of the MOEA

While for the second fitness function, the fitness score of the performance of the robot during the simulation will be evaluated. The main factor of the performance fitness is the evaluation of the travelled distance of each individual from the origin to the goal destination. The final distance of the individual from the goal destination is squared in order to increase the weight in the fitness function. Thus, the individual with shorter travelled distance will be severely penalized while successful individual that reaches goal will be greatly rewarded. The second part of the performance fitness is to penalize individuals that have collision with the obstacles during the simulation. The total number of collisions occurs during the simulation is divided by the maximum number of collision that is possible to occur in a single run of simulation in order to scale the penalize score with the fitness function. The mutation operation of the MOEA is similar with mutation operation of SOEA which has been described earlier.

2.3 Fabrication Methodology

One of the critical issue in evolutionary robotics is to transfer the simulation results into real world. High cost and long turnaround time of fabricating the robot parts are hindering researchers in transferring the simulation results into real world. In this research, a recent technology is accessed in fabricating the robot parts, which is by 3D printing technology. Fabrication cost of fabricating robots is considered high as the cost of manufacturing robots has to be absorbed in mass production [29]. Fabrication cost can be reduced with 3D printing as parts of the selected results to be fabricated with different sizes can be easily obtained by 3D printing.

2.3.1 3D printing technology

3D printing is a process of making three dimensional solid objects from a digital file. 3D printing may referred as Additive Manufacturing (AM). The creation of a 3D printed object is achieved using additive processes. In an additive process an object is created by laying down successive layers of material until the entire object is created. Each of these layers can be seen as a thinly sliced horizontal cross-section of the eventual object [30]. Difference from traditional ink-printing technology, 3D printing is capable to be done with a variety of materials. For example: plastics, glass, metal, polymers, wax, edible food, human tissue, sand & glue mixes, etc. 3D printing technology has been widely used in a lot of applications such as: design visualization, prototyping/computer-aided-design (CAD), architecture, metal casting, manufacturing, healthcare, entertainment and etc.

2.3.2 STL file generation for robot parts

Most of the available 3D printers required 3D model file in STL format to perform printing. Thus, robot parts that are needed to be fabricated have to be modeled and saved in STL file. There are three main parts of the robots that are needed to be fabricated by 3D printers which are the body, legs and wheels. A program has been designed in order to generate the STL file for 3D model of robot parts automatically.

Fig. 6 shows the examples of printable 3D models generated for robot parts. The 3D models generated are according to the defined input parameters with sockets which are ready to assemble with servos and sensors. Fig. 7 shows the printed robot parts.

2.3.3 Electronic components of real world SAWRs

The designed SAWR in this research consists of three main electronic components which are the sensors, servos and DC geared motors. Two sensors are installed in the real world SAWR where one is placed in the front as s1 in Fig. 1b and the other one is placed in the rear bottom as s2 in Fig. 1b. Servos are installed in SAWR in order to control the angle of legs while DC geared motors are installed in driving the SAWR to move forward.

There are two different sensors that have been chosen for the front sensor and rear sensor due to the difference in requirement of the measurement distance requirement for both sensors. The front sensor requires a longer distance for the maximum measurement distance while the back sensor requires a shorter distance for the minimum measurement distance. Therefore, the selected sensor for the front sensor is an infrared sensor with 4-30 cm sensing range and another infrared sensor with 2-8 cm sensing range for the rear sensor.

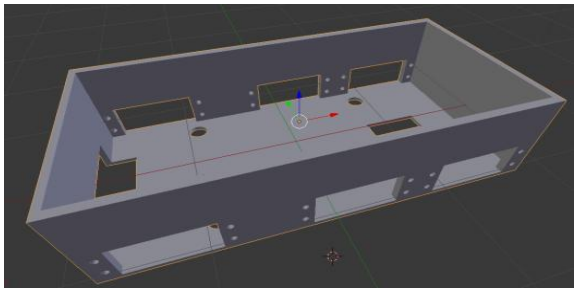

(a) Robot body

(b) Robot leg

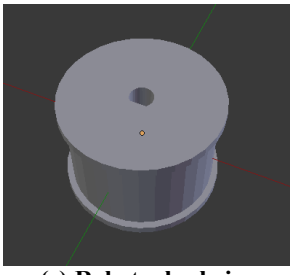

(c) Robot wheel rim

Fig. 6. 3D models generated for robot parts

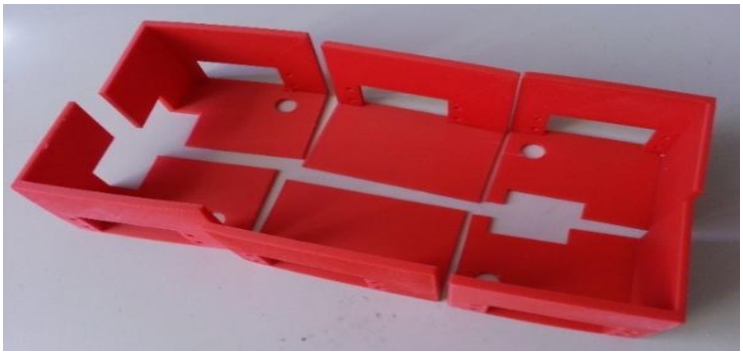

(a) Printed robot body

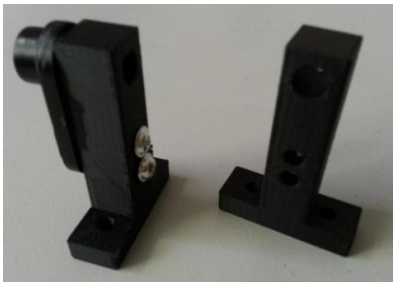

(b) Printed robot legs

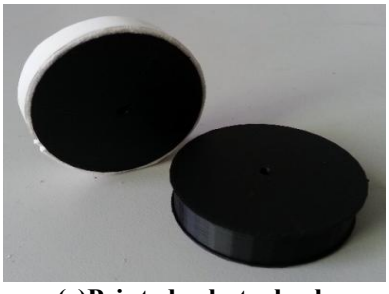

(c)Printed robot wheels

Fig. 7. Printed robot parts

On the other hand, the selection of servos and DC geared motors are based on the torque required to drive the SAWRs. The maximum weight for the biggest possible evolved SAWR is first calculated, which is

950 g. After the consideration of the longest possible evolved leg which is 10 cm, the minimum torque required for servos is 9.5 kg/cm. Therefore, a servo with 180 degree rotational angle and torque of 17 kg/cm is selected.

Since the original marching position of the SAWR is driven by six DC geared motors, the weight of the SAWR will be shared by all the motors. However, there are cases that the SAWR is moving forward with only four wheels during the climbing reconfiguration method. The total weight of the SAWR then is only divided by four and shared by four DC geared motors. Therefore, the minimum requirement of torque for each DC geared motor is 950 g divided by four, which is 0.238 kg. With the consideration of the largest possible evolved wheel radius, which is 40mm, the minimum torque required for each DC geared motor is 1.0 kg/cm. Thus, the selected DC geared motor for the SAWR is 1.8 kg/cm in torque and 45 RPM in rotational speed.

3 Experiment Setup and Results

3.1 Task Environment and Simulation Parameters Setup

Simulations of this research have been carried out with the Webots simulation software. Webots is a high fidelity physical-based robot simulation tool used to model, program and simulate mobile robots. Fig. 8 shows the task environment for this research. As can be seen from Fig. 8, the task environment is a multi-step environment. The first step is 50 mm in height, the stairs-like step is 55mm in height and the last step is 80 mm in height. The task for the robot in the environment is to travel from origin to goal by climbing over all the obstacles.

Each experiment is conducted with five runs in order to determine the efficiency of the algorithm in obtaining the optimized morphology of a climbing SAWR. Individuals are given 60 seconds to simulate for the simulation in multi-steps environment where the amount of time is obtained from preliminary experiments. The maximum number of generation for all experiments are 500 as preliminary experiments showed that optimized solutions are able to be obtained within 500 generations. Last but not least, the population size for each generation is one where one parent will produce one offspring for next generation. The summary of the simulation parameters setup are shown in Table 1.

Besides the setup for the simulation parameters, the parameter of the evolving objects has to be set too which is the maximum value and minimum value for each evolving object. The evolving objects parameter setup is presented in Table 2. The minimum value set for wheel radius is 15 mm, leg length is 35 mm and body length is 200 mm. All these values are chosen as these are the minimum values for the parts to be fabricated with 3D printer later. While the maximum value for wheel radius is 40 mm, leg length is 100 mm and body length is 350 mm. The maximum values are chosen with the consideration of measurement for the highest step in the task environment.

Table 1. Summary of simulation parameters setup

Parameter	Values
Runs	5
Simulation time (seconds)	60
Maximum number of generation	500
Population size	1

Table 2. Evolving objects parameter setup

Object	Wheel radius	Leg length	Body length
Minimum (mm)	15	35	200
Maximum (mm)	40	100	350

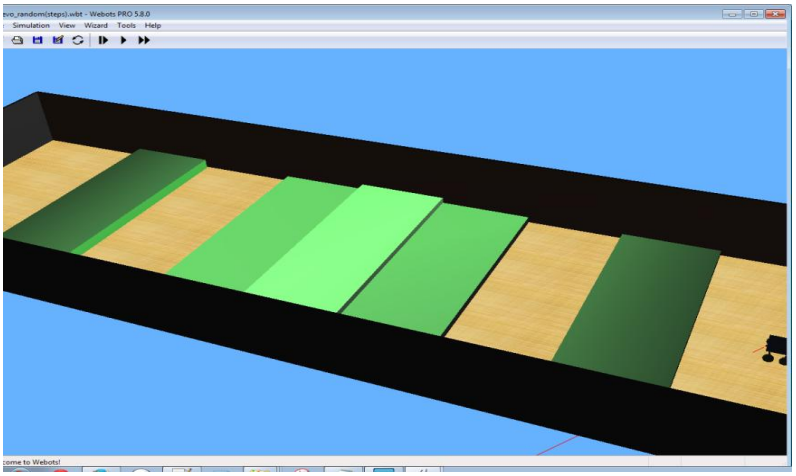

Fig. 8. Multi-steps task environment

3.2 Simulation Results

3.2.1 SOEA results

The results for the five runs of experiments with SOEA are shown in Table 3. From the results, each run of the experiment with SOEA is able to produce a climbing SAWR with optimized morphology. As can be seen from Table 3, solutions from the five runs of SOEA are approaching to optimum solutions as the fitness scores of the optimized solutions are closed to each other. Fig. 9 shows the optimized solutions which are climbing SAWRs with optimized morphology in simulation software. Fig. 10 shows the fitness score of fittest individual over generations for five runs of SOEA experiments.

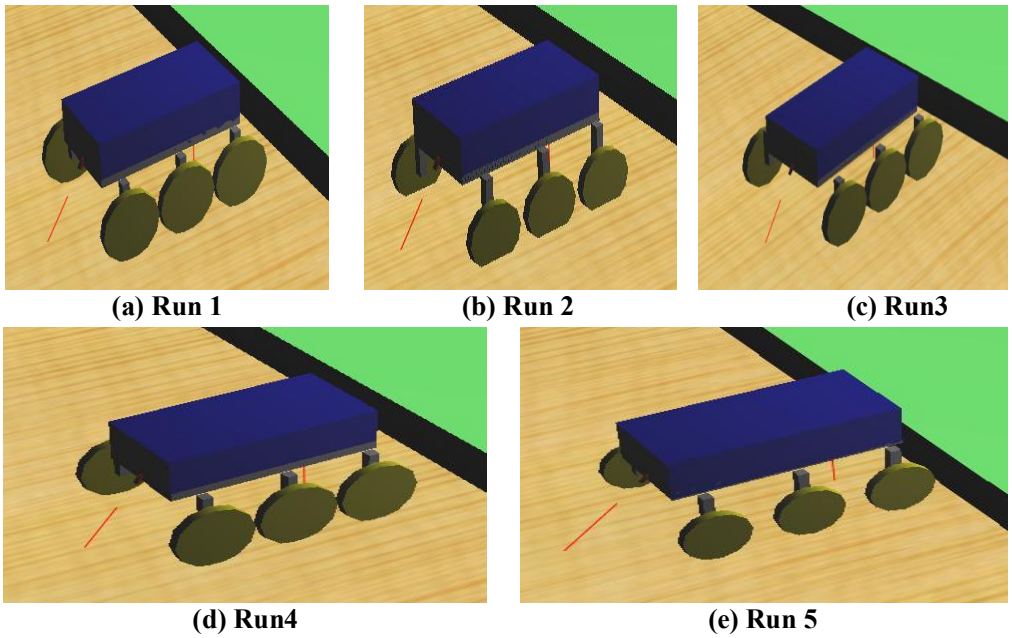

(a) Run 1 **(b) Run 2** **(c) Run3**

(d) Run4 **(e) Run 5**

Fig. 9. Optimized solutions for each run in simulation software

Table 3. Optimized solutions for five runs of SOEA

	Run 1	Run 2	Run 3	Run 4	Run 5
Fitness score	0.298	0.299	0.298	0.292	0.305
Body length (mm)	206	200	209	200	216
Leg length (mm)	52	64	49	54	57
Wheel radius (mm)	40	35	40	38	32
Distance from goal	0	0	0	0	0
Collisions	0	0	0	0	0

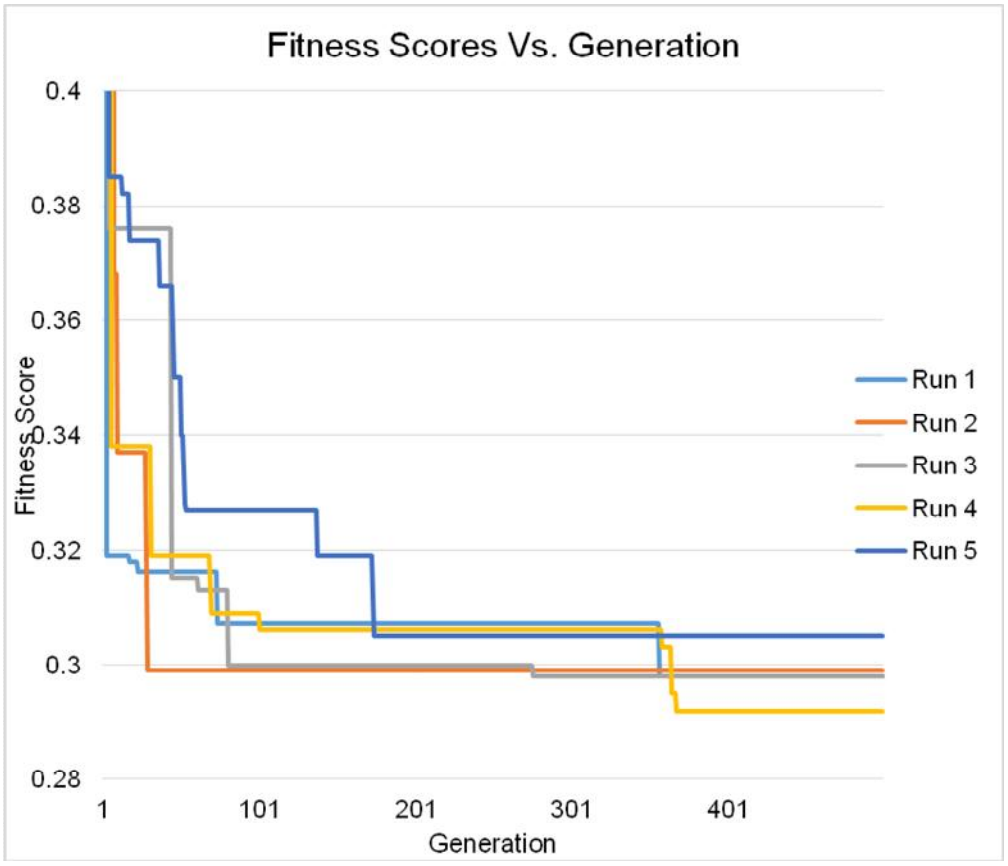

Fig. 10. Fitness scores vs. generation for five runs

3.2.2 MOEA results

From the experiments, each run of MOEA is able to produce a set of Pareto optimal solutions. In this paper, the result presentation is only presented for one run of MOEA experiment. The graph of the Pareto-set optimal solutions is presented in Fig. 11. The graph of Pareto-set optimal solutions is divided into few regions based on the achievement of the individual SAWR. For example, solutions in region one have the worst performance where they are not able to perform any climbing motion while solutions in region four are the best in performance fitness where they can complete the task environment by climbing all the steps. One solution from each region is selected for presentation. Detailed descriptions for each selected optimal solution are presented in Table 4. Fig. 12 shows the selected solutions of the Pareto set of optimal solutions in simulation.

Table 4. Detailed description of selected solutions from Pareto-set optimal solutions

	Solution a	Solution b	Solution c	Solution d
Size fitness	0.25	0.257	0.264	0.312
Body length (mm)	200	200	200	215
Leg length (mm)	35	37	41	65
Wheel radius (mm)	15	20	23	32
Performance fitness	25.16	13.65	1.72	0
Distance from goal	5.015912	3.693954	1.310031	0
Collisions	0	0	0	0

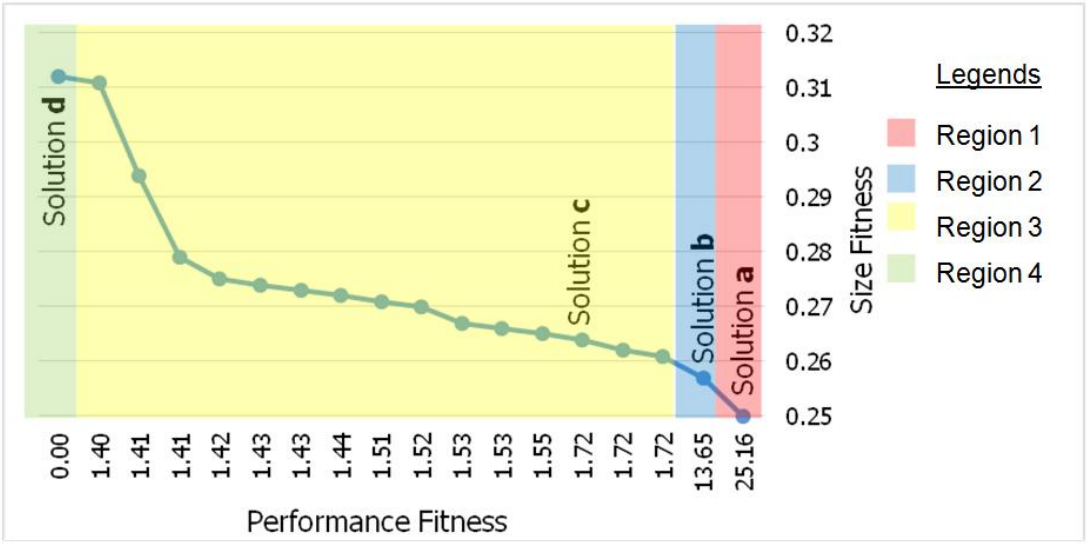

Fig. 11. Pareto-set optimal solutions

3.3 Fabricated Real World SAWRs

For the fabrication, an optimized solution from SOEA experiment and selected solutions from a Pareto-set optimal solution of MOEA experiment are chosen. In this research, optimized solution from Run 5 of SOEA and selected solutions from Pareto-set optimal solutions of MOEA which are Solution **a**, Solution **b**, Solution **c** and Solution **d** that are presented in previous section are selected to be fabricated. Fig. 13 shows the fabricated real world SAWRs based on the selected optimal solutions from SOEA and MOEA.

3.4 Real World Testing of Fabricated SAWRs

The accuracy of the fabricated real world SAWRs in comparing to the SAWRs in simulation are rated based on the performance of the fabricated real world SAWRS in performing climbing motion in real world environment. The accuracy is evaluated based on formula shown in equation 7. Since the main objective of this research is to obtain an optimized SAWR with climbing ability, thus higher percentage which is 70% of the accuracy is credited based on the climbing ability. While the remaining 30% is credited based on the overall performance evaluation of the fabricated real world SAWRs in performing the climbing motion and interacting with the environment.

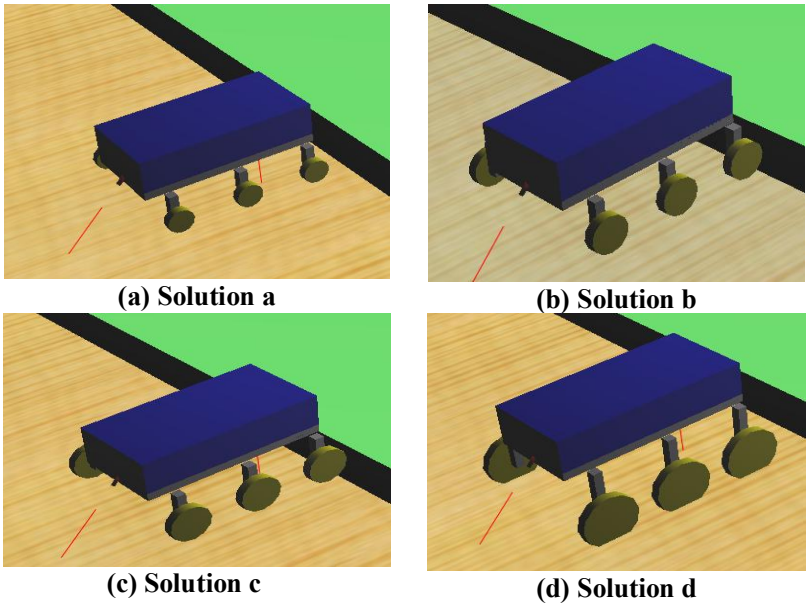

Fig. 12. Selected solutions of pareto-set optimal solutions in simulation software

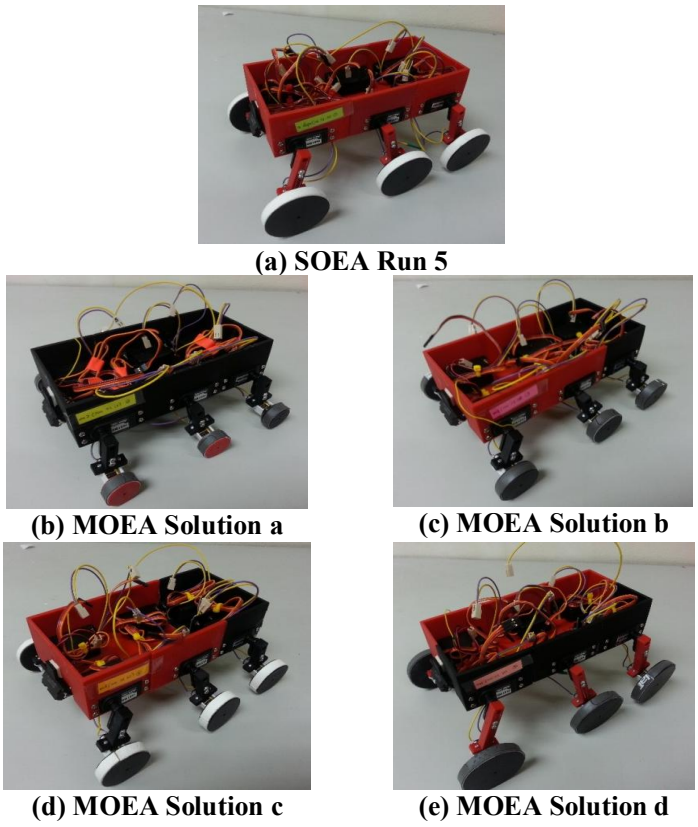

Fig. 13. Fabricated real world SAWRs

Accuracy = Climbing Ability (70%) + Overall Performance (30%) (7)

Fig. 14 shows the example of fabricated real world SAWR (SOEA Run 5) performs climbing motion over stair-like steps. From the figure, fabricated real world SAWR is able to perform climbing motion over stair-like steps as how the SAWR performs climbing motion in simulation.

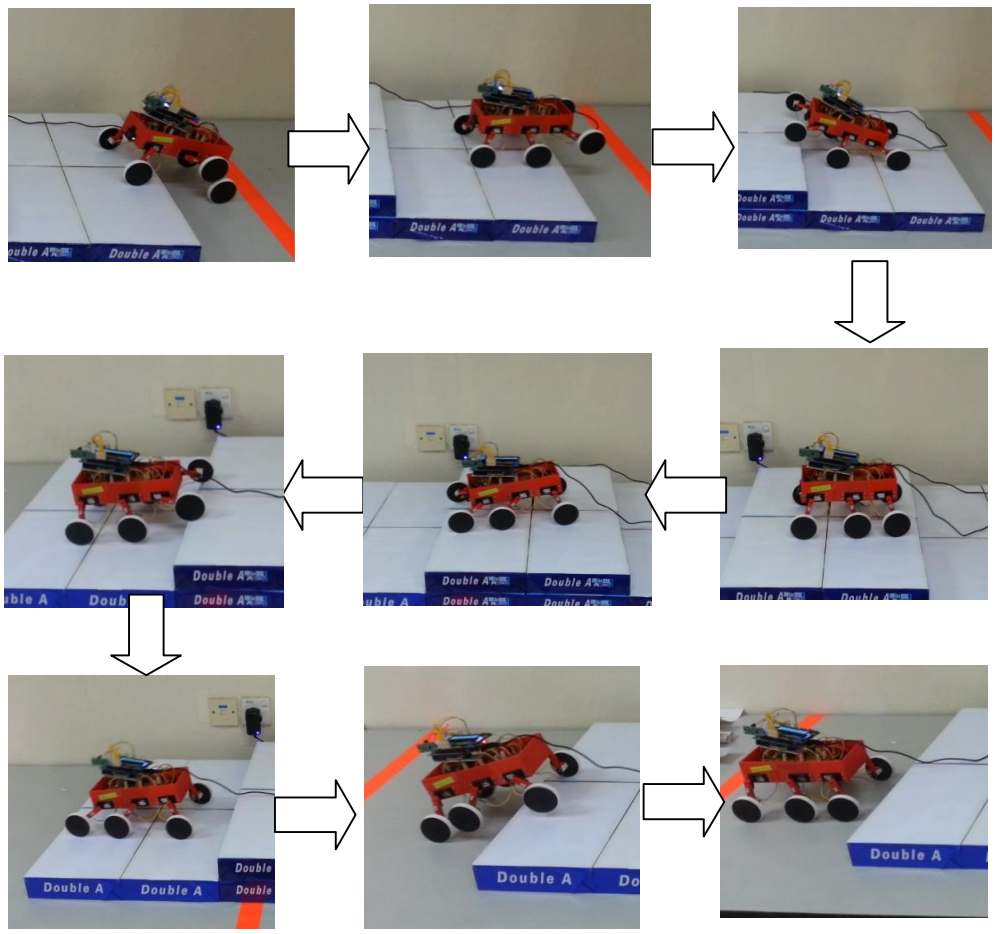

Fig. 14. Fabricated real world SAWR performing climbing motion

Table 5 shows the accuracy of all the fabricated real world SAWRs compared to SAWRs in simulation. The accuracy calculation is based on Equation 7 which has been explained previously. From the results, each fabricated real world SAWR is able to climb over the obstacles that it is managed to climb over in the simulation. All the obstacles designed in the real world task environment are exactly the same in height with all the obstacles in the simulation task environment. Therefore, the climbing ability for all the fabricated real world SAWRs are credited with full score. For the overall performance, each fabricated real world SAWR is credited based on the degree of defect during the climbing performance. In general, defects of the climbing performance are caused by the distortion of direction of the fabricated real world SAWRs during the operation in real world environment. In the simulation, all the SAWRs are able to march forward in a straight line after performing climbing motion. The defection is speculated as the servos of fabricated real world SAWRs are not turning synchronously as in simulation.

Table 5. Accuracy of fabricated real world SAWRs compared to SAWRs in simulation

SAWR	Climbing ability (70%)	Overall performance (30%)	Accuracy (100%)
SOEA run 5	70%	20%	90%
MOEA solution a	70%	25%	95%
MOEA solution b	70%	20%	90%
MOEA solution c	70%	15%	85%
MOEA solution d	70%	10%	80%

4 Conclusions

In this research, an artificial evolution method in designing and optimizing the morphology of a climbing SAWR has been proposed. Results show that the proposed evolution with SOEA in this research is able to produce climbing SAWRs with optimized which is smallest possible morphology. On the other hand, the proposed evolution with MOEA is able to produce a Pareto-set of optimal solutions which are different sizes of SAWR with different levels of achievement in performing the climbing motion. The optimal solutions obtained from the evolution are then transferred into real world SAWRs with 3D printing technology. Fabricated SAWRs are then assembled with servos and sensors and the ability of each fabricated real world SAWR in performing climbing motion is evaluated. Results show that overall accuracy of the fabricated real world SAWRs in comparing to the evolved solutions in simulation is rated at 85.8%. All the fabricated real world SAWRs are able to complete the task environment which are the climbing motion that is designed in the simulation.

With the results finding from this research, future work should be focusing on looking for more opportunity to apply artificial evolution method in designing robots. Results from this research are again proven that artificial evolution method is able to help human designers in designing and optimizing morphology of robots. The artificial evolution method is not only limited in designing and optimizing the morphology of robots, future work can be done in co-evolving the morphology as well as the controller of the robots for a comprehensive evolution process. Besides that, investigation can be done on releasing the constraints of current research by evolving more objects. In this research, the evolution is only done on three objects which are the length of robot body, length of robot legs and radius of robot wheels. Suggested objects that can be involved in the evolution of future work are the coordinate of sensors and legs placement. The placement of sensors and legs in current research are fixed. Evolving the placement of sensors and legs is foreseen to produce different and might be better optimized solutions. On the other hand, the task environment for the evolution process can be further improved to a more challenging environment in the future work; which may include uneven terrain and steps. Last but not least, realization of real world robots from evolved solutions using 3D printing has been proven workable. In this research, selected evolved solutions are successfully fabricated into real world SAWRs by 3D printing technology with minimum fabrication cost and turnaround time. Therefore, the methodology of robot fabrication with 3D printing technology can be used or referred in the future.

Acknowledgements

This research was funded under Science Fund project SCF0085-ICT-2012 granted by the Ministry of Science, Technology and Innovation, Malaysia.

Authors' Contributions

This research and manuscript were prepared by author SHL under supervision of author JT. Both authors read and approved the final manuscript. This is an expanded paper of "Integrating Evolutionary Robotics with 3D printing for Rapid Fabrication and Deployment of a Physically-Simulated Autonomous Six

Articulated-Wheeled Robot" [31]. This paper includes the presentation of evolution with MOEA and a more detailed presentation of the real world SAWRs' fabrication and testing.

Competing Interests

Authors have declared that no competing interests exist.

References

[1] Ong CH, Shamsudin HM, Amin A. Biologically inspired hybrid three legged mobile robot. Student Conference on Research and Development. 2002;181-183.

[2] Shen S, Li C, Cheng C, Lu J, Wang S, Lin P. Design of a leg-wheel hybrid mobile platform. IEEE International Conference on Intelligent Robots and Systems. 2009;4682-4687.

[3] Matsumoto O, Kajita S, Komoriya K. Flexible locomotion control of a self-contained biped leg-wheeled system. Proceedings of the 2002 IEEE/RSJ International Conference on Intelligent Robots and Systems. 2002;2599-2604.

[4] Matsumoto O, Kajita S, Saigo M, Tani K. Biped-type leg-wheeled robot. Advanced Robotics. 1999;13(3):235-241.

[5] Ylönen SJ, Halme AJ. Work partner – centaur like service robot. Proceedings of the 2002 IEEE/RSJ International Conference on Intelligent Robots and Systems. 2002;727-732.

[6] Ota Y, Yoneda K, Tamaki T, Hirose S. A walking and wheeled hybrid locomotion with twin-frame structure robot. Proceedings of the 2002 IEEE/RSJ International Conference on Intelligent Robots and Systems. 2002;2645-2651.

[7] Hirose S, Takeuchi H. Study on roller-walker (Basic characteristics and its control). Proceedings of the 1996 IEEE International Conference on Robotics and Automation. 1996;3265-3270.

[8] Endo G, Hirose S. Study on roller-walker (Multi-mode steering control and self-contained locomotion). Proceedings of the 2000 IEEE International Conference on Robotics and Automation. 2000;2808-2814.

[9] Manuel F, Silva JA, Tenreiro M. A literature review on the optimization of legged robots. Journal of Vibration and Control. 2012;1753-1767.

[10] Tadakuma K, Tadakuma R, Maruyama A, Rohmer E, Nagatani K, Yoshida K, Ming A, Makoto S, Higashimori M, Kaneko M. Armadillo-inspired wheel-leg retractable module. IEEE International Conference on Robotics and Biomimetics. 2009;610-615.

[11] Smith J, Sharf I, Terntini M. PAW: A hybrid wheeled-leg robot. Proceedings of the IEEE International Conference on Robotics and Automation. 2006;4043-4048. Orlando, Florida.

[12] Lim SH, Teo J. Recent advances on locomotion mechanisms of hybrid mobile robots. WSEAS Transactions on Systems. 2015;11-25.

[13] Akerka R. Introduction to artificial intelligence. PHI Learning Pvt. Ltd; 2005.

[14] Endo K, Yamasaki F, Maeno T, Kitano H. Co-evolution of morphology and controller for biped humanoid robot. In Kaminka A. Gal, Lima U. Pedro, R. Rojas. RoboCup 2002: Robot Soccer World Cup VI. Springer; 2003.

[15] Lee W. An evolutionary system for automatic robot design. IEEE Internatonal Conference on Systems, Man, and Cybernatics. 1998;(4):3477-3482.

[16] Wang L, Tan K, Chew C. Evolutionary robotics: From algorithms to implementations. World Scientific Publishing; 2006.

[17] Leger C. DARWIN2K - An evolutionary approach to automated design for robotics. Kluwer Academic Publishers; 2000.

[18] Nol S, Floreano D. Evolutionary robotics - The biology, intelligence, and technology of self-organizing machines. The MIT Press; 2000.

[19] Jurez-Guerrero J, Muoz-Gutirrez W, Cuevas WM. Design of a walking machine structure using evolutionary strategies. Proc. of the IEEE Int. Conf. on Systems, Man and Cybernetics. 1998; 1427-1432.

[20] Ishiguro A, Kawasumi K, Fujii A. Increasing evolvability of a locomotion controller using a passive dynamic-walking embodiment. Proc. of the IEEE/RSJ Int. Conf. on Intel. Robots and Systems. 2002; 2581-2586.

[21] Lipson H, Pollack JB. Towards continuously recon-figurable self-designing robots. Proc. of the IEEE Int. Conf. on Rob and Aut. 2000;1761-1766.

[22] Endo K, Yamasaki F, Maeno T, Kitano H. A method for co-evolving morphology and walking pattern of biped humanoid robot. Proc. of the IEEE Int. Conf. on Rob and Aut. 2002;2775-2780.

[23] Endo K, Maeno T, Kitano H. Co-evolution of morphology and walking pattern of biped humanoid robot using evolutionary computation - consideration of characteristic of the servomotors. Proc. of the IEEE/RSJ Int. Conf. on Intel. Robots and Systems. 2002;2678-2683.

[24] Endo K, Maeno T. Co-evolution of morphology and walking pattern of biped humanoid robot using evolutionary computation - designing the real robot. Proc. of the IEEE Int. Conf. on Rob and Aut. 2003;1362-1367.

[25] Manuel F, Silva, Ramiro S, Barbosa JA, Tenreiro M. Optimization of hexapod locomotion using genetic algorithms. Proceedings of the Conference MIC 2010 – The 30th IASTED International Conference on Modelling, Identification and Control. 2010;291-297.

[26] Rommerman M, Kuhn D, Kirchner F. Robot design for space missions using evolutionary computation. IEEE Congress on Evolutionary Computation (CEC). 2009;2098-2015.

[27] Kadota T, Yasuda T, Matsumara Y, Ohkura K. An incremental approach to an evolutionary robotic swarm. IEEE/SICE International Symposium on System Integration (SII). 2012;458-463.

[28] Lu J, Bu C. Study on the mobile robot reconfiguration control methods. IEEE International Conference on Automation and Logistics. 2009;2045-2049.

[29] Lipson H, Pollack JB. Automatic design and manufacture of robotic life forms. Nature. 2000;974-978.

[30] Anonymous. What is 3D printing? 2015. Accessed 13 January 2015.
Available: http://3dprinting.com/what-is-3d-printing

[31] Lim SH, Teo J. Integrating evolutionary robotics with 3D printing for rapid fabrication and deployment of a physically-simulated autonomous six articulated-wheeled robot. Proceedings of the International Conference on Artificial Intelligence and Pattern Recognition. 2014;184-191.

Peer-review history:
The peer review history for this paper can be accessed here (Please copy paste the total link in your browser address bar)
http://sciencedomain.org/review-history/9920